

## RESEARCH ARTICLE

# Classifying and Localizing Abnormalities in Brain MRI Using Channel Attention Based Semi-Bayesian Ensemble Voting Mechanism and Convolutional Auto-Encoder

SYED MUHAMMAD AHMED HASSAN SHAH<sup>1</sup>, ASAD ULLAH<sup>1</sup>, JAWAID IQBAL<sup>2</sup>, SAMI BOUROUIS<sup>3</sup>, SYED SAJID ULLAH<sup>4</sup>, SADDAM HUSSAIN<sup>5</sup>, MUHAMMAD QASIM KHAN<sup>1</sup>, YASER ALI SHAH<sup>1</sup>, AND GHULAM MUSTAFA<sup>6</sup>

<sup>1</sup>Department of Computer Science, COMSATS University Islamabad, Attock Campus, Attock 43600, Pakistan

<sup>2</sup>Faculty of Computing, Riphah International University, Islamabad 45210, Pakistan

<sup>3</sup>Department of Information Technology, College of Computers and Information Technology, Taif University, Taif 21944, Saudi Arabia

<sup>4</sup>Department of Information and Communication Technology, University of Agder (UiA), 4898 Grimstad, Norway

<sup>5</sup>School of Digital Science, Universiti Brunei Darussalam, Jalan Tungku Link, Gadong BE1410, Brunei

<sup>6</sup>Department of Computer Science, Shifa Tameer-e-Millat University, Islamabad 44000, Pakistan

Corresponding author: Syed Sajid Ullah (syed.s.ullah@uia.no)

This work was supported by the Deanship of Scientific Research, Taif University.

**ABSTRACT** Adults who have brain tumors face a serious and potentially fatal challenge since the tumors rapidly growing malignant cells can seriously impair their physiological ability. In clinical practice, imaging techniques such as MRI, PET, and CT scans are widely used to determine the size, kind, and location of tumors. The goal of this research is to create a Computer-Aided Diagnostic (CAD) system that can automatically segment and classify brain tumors utilizing T1W-CE Magnetic Resonance Imaging (MRI) of the brain. The CAD system will involve two primary tasks: tumor classification, which determines the type of tumor depicted in the image, and tumor segmentation, which involves accurately determine the tumor region from the surrounding healthy tissue. By automating these processes, the proposed system aims to enhance the accuracy and effectiveness of brain tumor diagnosis and treatment planning. The classification of brain tumors into multiple classes is recognized as a complex challenge within the field of medical imaging. This research article proposes a model named VS-BEAM that can be used efficiently for clinical decision-making. The proposed VS-BEAM (Voting Based Semi-Supervised Bayesian Ensemble Attention Mechanism) model has been examined for a brain tumor's multi-class classification. The VS-BEAM model achieved the highest level of accuracy possible. The proposed work achieves maximum sensitivity, specificity, and diagnostic accuracy compared to existing models using T1W-CE MRI images. A convolutional autoencoder is utilized for extracting tumors from MRI images. The accuracy obtained from testing data of 264 brain tumors was 98.91%, indicating that the method is effective and can be used in the clinical context to assist in detecting larger or even smaller tumors.

**INDEX TERMS** Magnetic resonance imaging, medical imaging, squeeze and excitation networks, Bayesian learning, ensemble learning, convolutional autoencoder, directed acyclic graph (DAG) network, brain tumors.

## I. INTRODUCTION

Diagnosing a tumors comprises the characterization of the abnormal cells [1], e.g., whether they are cancerous or

The associate editor coordinating the review of this manuscript and approving it for publication was Fu-Kwun Wang<sup>1</sup>.

noncancerous. Tumors can be characterized by size, location and other factors that affect clinical appearance. Cancer, a disease that normally develops in adulthood, is characterized by abnormal growth of cells that can invade other tissues and cause serious harm. Signifying different types of cancer cells and the tumor they cause; brain tumors may be either primary

or metastatic. Tumors in the brain and central nervous system are often hard to treat. The primary tumors include (1) meningioma, which is in the defensive layer enclosing the brain and vertebral canal; (2) glioblastoma, which develops from cells of neural crest and occurs more commonly at a younger age than meningiomas; (c) Pituitary tumor, which originates from the pituitary gland [2]. Meningioma brain tumors are noncancerous tumors arising from the tissue layer bordering the brain and vertebral canal. Pituitary tumors are one of the rarest brain tumors in humans [2].

Medical Radiology diagnoses or provides information about a person's health. The most common types of medical imaging are internal medicine X-rays, CT scan imaging, MRI (Magnetic Resonance Image), ultrasounds, and PET scan imaging. These methods provide an anatomical view of the body, which may be used to identify illnesses and injuries besides monitoring disease progression. Structural and functional MRI scans provide detailed imaging of brain tumors. T1-w and T2-w contrast-enhanced brain MRIs are beneficial in screening brain neoplasms.

An accurate diagnosis is the first step towards effective cancer treatment. Medical disciplines such as radiotherapy and chemotherapy are used for the operative handling and treatment of patient's malignant diseases. The treatment process selection depends on neoplasm types, position, size, etc. The manual treatment of a brain neoplasm is challenging, and the principal challenge is determining the size and shape of a tumor. Computer Aided Diagnosis (CAD) system for Brain neoplasm segmentation and classification is necessary to automatically classify brain tumors using large-scale MRI image sequences [3].

The existing literature on brain tumor classification and segmentation identifies several research gaps, including the challenges of dealing with class imbalance data, limited data availability, and the inadequacy of current architectures for effective tumor diagnosis. These gaps create obstacles to achieving high levels of accuracy and efficiency in diagnosis. Furthermore, managing class imbalance datasets can be challenging. As a result, there is a need for new architectures and techniques to enhance the performance of categorization and segmentation of brain tumors models.

Owing to the complexity of the brain's anatomy and the tumor's variability, classification and segmentation of brain tumors has proven to be a difficult issue in medical imaging. The accuracy and effectiveness of the conventional approaches are constrained. The deep ensemble learning-based VS-BEAM model uses an ensemble of three different classifiers, including a Bayesian classifier, a modified dense classifier, and a traditional dense network classifier, in an effort to close these gaps. The classification and segmentation of brain tumors in MRI images can now be done with greater accuracy and efficiency thanks to the application of ensemble learning. The model offers a novel approach for ongoing clinical studies for computer-assisted brain tumor diagnosis. This article uses an ensemble deep learning framework titled VS-BEAM to investigate the gap in precise brain tumor

classification and segmentation. The paper adds value by proposing a system that achieves high performance in classifying and segmenting brain tumors in MRI images, which can aid in computer-aided diagnosis and potentially improve patient outcomes.

Tumor classification has received growing interest in recent years. In this research work, we propose a CAD system for the automatic segmentation and classification of intracranial tumors. The proposed approach classifies and segments the brain tumors from the T1W-CE MRI sequences. Brain MRI sequences consist of three types of neoplasm Meningioma, Glioma, and Pituitary neoplasm. The T1W-CE MRI dataset is used to evaluate the VS-BEAM model which is available on the Figshare platform. To enhance the performance of the proposed model, pre-processing is performed to normalize and resize the data. The brain MRIs are split into 9:1, i.e., 90% of the brain MRIs are considered training sets, while the remaining 10% are used for testing.

For the identification of accuracy, we have compared the segmented tumor with a ground truth mask. We used a Convolutional Autoencoder (CAE) with latent space clustering techniques to compare segmentation accuracy. The CAE trained on the ground truth mask generates a probability for each pixel in the segmented tumor region and marks all pixels as "present" or "absent" from that segmentation. This is performed using a pixel-wise error measure by comparing the probability distribution with our segmentation model. CAE is a feature extraction technique which explicitly encodes the covariance matrix of a set of images, where each pixel corresponds to a training point in the data. The CAE is trained using a few samples to pass through its recurrent layers. The resulting model presents an array consisting of multidimensional representations of data points.

This paper introduces a novel approach for classifying brain tumors that combines multiple learning mechanisms, including Squeeze and Excitation Attention, Bayesian Learning, a Convolutional Network, and Ensemble Learning. Our proposed system was tested on the Figshare dataset and demonstrated impressive performance. The key contributions of this research are as follows:

- A novel computer-aided diagnosis algorithm named VS-BEAM has been introduced to diagnose brain tumors. The ensemble architecture integrates multiple models to predict the presence of tumors in MRI images. The algorithm uses voting mechanism to determine the final abnormality, which improves the efficiency and accuracy of diagnosis. We integrate Squeeze and Excitation (SE) Attention Blocks in the CNN (Convolutional Neural Network) network for efficient feature extraction. we concluded that combination of SE attention with CNN is more coherent than only CNN networks.
- The VS-BEAM algorithm uses ensemble learning with different classifier algorithms. One is a classical dense network that solves the problem as a multiclass classification, while the second is also a dense classifier but tackles the multiclass brain tumor classification problem

as three binary class classification problems. Finally, the third classifier is a Bayesian classifier that classifies the tumor by estimating the posterior distribution.

- The proposed system for classifying and segmenting brain tumors in MRI images achieves high-performance measures in the evaluation phase. The end-to-end model demonstrated promising results and has the potential to be used in active clinical trials for computer-aided brain tumor diagnosis.

The main motivation of utilizing deep learning for classifying and segmenting of brain tumors is to enhance the precision and efficiency of patient diagnosis and treatment planning. Deep learning techniques have shown tremendous potential in providing automated and precise solutions for processing medical images, including essential tasks including tumor segmentation and classification. Healthcare practitioners can speed up and standardize their decision-making processes through the automation of certain procedures, resulting in more quick and reliable patient care. Deep learning algorithms may also recognize tiny abnormalities and complex patterns in medical images that might escape human inspection, resulting in more precise diagnosis and better patient outcomes. This could reduce the amount of work that doctors have to do and improve the general standard of treatment.

The remainder of the paper is structured as follows: Section II examines the literature work. Section III exhibits the idea of this research and recommends the proposed methodology. Section IV provides the experimental arrangement, results and discussion. Finally, Section V concludes the work and presents several guidelines for future analysis.

## II. RELATED WORK

The related work is divided into two subsections i.e., Brain tumor classification and Brain Tumor Segmentation.

### A. BRAIN TUMOUR CLASSIFICATION

In the literature, multiple techniques are available for the classification and segmentation of tumors. A fuzzy C Means (FCM) technique is used to extract the neoplasm regions and then the Probabilistic Local Ternary Patterns algorithm is implemented to get the neoplasm substructure [4]. For classification of the neoplasm on extracted slices, support vector machine (SVM) is employed. The segmentation approach achieves a dice index of 76% on BraTS 2013 while the dice value of 81% is achieved for BraTS 2015 for the whole neoplasm. Convolutional Network is used to classify the neoplasms of the pituitary, glioma and meningioma achieving the accuracy of 94.39%.

Transfer learning is widely used for computer vision problems like detection, segmentation, etc. The transfer learning approach is used for segmentation of brain tumor and classification by Ellah et al. [5]. The CNN architecture consists of AlexNet, VGG16, and VGG19 deep learning models. This transfer learning mechanism is used to localize the tumor in MRI images. The model achieves an accuracy

of 99.55% on the RIDER Neuro MRI images. The classification is done by using many different algorithms via transfer learning like GoogleNet, AlexNet, SENet, VGG-16, ResNet-18, ResNet-50, ResNet-101, VGG-19 among others. 98.71% classification accuracy is obtained on T1w contrast-enhanced brain MRI. On the other hand, 0.87% dice index is accomplished with 804 3D MRIs (From BraTS 2013).

A Deep Learning (Convolutional Neural Network) approach is used for 3 types of neoplasm classification [6]. 99.3% accuracy is obtained in binary classification (neoplasm/non-neoplasm). The multi-class classification process by Gupta et al. [7] obtains 92.66% accuracy measure.

CNN is vastly used in image classification problems. A similar technique is introduced by Francisco et al. [8] in 2021. A deep Convolutional network for computerized diagnosis of brain Neoplasm is used. Neoplasm types are classified with 97.3% accuracy and three million (2,856,932) trainable parameters. The dice index (used as the performance measure) is 82.2% with an average recall of 0.940 and 0.967 pttas value on 3064 T1-weight MRI.

Stacked connections of layers cause overfitting in deep learning. The network memorizes data instead of generalizing it. Therefore, to tackle the vanishing gradient problems in brain Neoplasm classification, Lokesh et al. [9] proposed a Residual Learning (ResNet-50) technique in 2021. For classification purposes, binary cross entropy and stochastic gradient decent SGD optimizer with learning rate of 0.001 is used. The accuracy of 97.08% with data augmentation and accuracy of 97.48% without it was attained on the brain dataset consisting of 3064 MRIs.

A CNN-based dense EfficientNet classification of brain neoplasm is presented in [10]. Different dense and dropout layers are added in the Efficient Network for modification purposes. 98.78% accuracy was achieved with data augmentation on 3260 T1-w contrast enhanced brain MRI.

Deep transfer learning is used for efficient features extraction in images data. Pre-trained Darknet architecture (DarkNet-19 and DarkNet-53) with two-level wavelet decomposition and different image operations like rotation and scaling are used for tumor classification. They classify and segment neoplasm from T1-weighted CE MRI. The Darknet architecture obtained training accuracy measure of 99.60% and 98.54 testing accuracy measure [11], [12]. The Two-Dimensional Super pixel technique is used for segmentation with a dice index of  $0.94 \pm 2.6\%$ .

Recent research in BMC Medical Informatics and Decision Making proposed deep learning and machine learning approaches for early detection and classification of brain tumors, including glioma, meningioma, and pituitary gland tumors, using MRI brain images [13]. They utilized a dataset of 3264 MRI brain images and applied preprocessing and augmentation algorithms to them. The study introduced a convolutional auto-encoder network and an innovative 2D convolutional neural network. The 2D CNN comprised multiple convolution and pooling layers and achieved a training accuracy of 96.47%, while the auto-encoder network had a

training accuracy of 95.63%. Additionally, six machine learning techniques were evaluated, and K-Nearest Neighbors (KNN) attained 86% accuracy. The study concludes that the 2D CNN achieves best accuracy in brain tumors classification and is less complicated than the auto-encoder network, which makes it suitable for clinical systems.

Shemanto et al.'s study focused on the difficulties of manually classifying brain tumors in medical image processing, as this can result in inaccurate diagnoses and prognoses [14]. The study suggested a thresholding method and used a HOFiler to preprocess 2D MR brain pictures. The goal of this preprocessing stage was to remove brain cancers and get the images ready for the future tumor segmentation. To precisely segregate tumors from MRI images, the team also used edge detection, segmentation, and morphological approaches. The proposed model outperformed the performance of other approaches looked at in the study, achieving a remarkable accuracy of 96.46% and precision of 96.19%. The use of HOFiler was found to be beneficial in achieving better results. Overall, the study presents a promising approach for accurate and efficient brain tumor segmentation in medical image processing.

The manual categorization of brain tumors in MRI images is difficult and requires the expertise of experienced radiologists and existing classification methods have unsatisfactory performance and computational costs. The research by El Wahab et al. [15], suggested the BTC-fCNN classification method, which uses deep learning to quickly and accurately identify between three different forms of brain tumors. Utilizing retrained five-fold cross-validation, the suggested approach attained average accuracy of 98.63% and 98.86% overall accuracy. Compared to other well-known convolutional neural networks (CNN), the BTC-fCNN model fared better. A potential method for precise and effective brain tumor classification in medical imaging is presented in the study.

Rasool et al. [16], used MRI scans and a cutting-edge hybrid deep learning CNN-based system to categorize three distinct types of human brain tumors. The technique uses deep learning and CNN in combination to classify data, with experiment results showing an accuracy of 98.7% when using an SVM classifier and SqueezeNet as a feature extractor, and an accuracy of 96.5% when using a finely tuned SqueezeNet model. The proposed system aims to assist in the non-invasive diagnosis of brain tumors.

Zhang et al. conducted a study to develop a radiomics pipeline using multiparametric-MRI to classify three types of brain tumors and predict their corresponding Ki-67 labeling index [17]. Their developed radiomics models accurately classified glioblastoma, metastasis, and primary central nervous system lymphoma and predicted Ki-67LI. These models can aid in treatment planning for brain tumors. The most important mask for tumor classification was the entire tumor, but the most important mask for Ki-67LI prediction was the tumor core. CE-T1WI was the most effective single modality

for all classifiers. The tri-categorized brain tumor assisted diagnosis model and Ki-67LI prediction model were built using the best feature sets and ELM, and both models performed well on the training and test datasets. The models for tri-categorized brain tumor aided diagnosis and Ki-67LI prediction achieved high performance, with an AUC of 0.96 (95% CI: 0.93, 0.99) and 0.96 (95% CI: 0.94, 0.98) on the training dataset, and 0.93 and 0.91 on the test dataset, respectively.

Another study is conducted by Hustinx et al. This study's objective is to assess the significance of calculating the standardized uptake value (SUV) in brain tumors using FDG PET images  $(\dots)(\dots)(\dots)$  [18]. The study included two groups: 20 normal subjects and 27 patients with malignant primary CNS tumors. SUV, tumor to cortex (T/C), and tumor to white matter (T/WM) activity ratios are computed. No connection could be made between whole-brain glucose cerebral metabolic rates (wCMRs) and SUVs. In the second group, there was no discernible difference between the SUVs in tumors and the contralateral cortex, and SUVs were often higher in tumors compared with the contralateral white matter. However, there existed substantial convergence between values, making it difficult to differentiate between malignant and nonmalignant tumors. T max/WM and T max/C, respectively, had activity ratios with sensitivity values of 74% and 96%. The most trustworthy techniques for assessing brain tumors presently are visual evaluation and activity ratio measurements.

Abdel Naser et al. conducted a study to evaluate the efficiency of MR spectroscopy (MRS) in classifying brain tumors. The study involved 22 patients having primary brain tumors who underwent MRS [19]. The metabolite ratios of Cho/NAA, Cho/Cr, Cho+Cr/NAA, and LL/Cr were computed at both short and intermediate echo times (TEs), while mI/Cr was computed only at short TE. The tumors were divided into low and high-grade groups based on histology, and a receiver characteristic analysis was employed to establish the cutoff values among the tumors. The accuracy, specificity and sensitivity of the resulting metabolite ratios were also calculated. The study findings indicated that high-grade tumors had considerably higher Cho/Cr, Cho+Cr/NAA and Cho/NAA ratios at intermediate TE compared to low-grade tumors. At short TE, high-grade tumors had considerably greater LL/Cr and Cho/Cr ratios compared to low-grade tumors. Using both TEs together produced a diagnosis accuracy of 88%. Cho/Cr, Cho+Cr/NAA, Cho/NAA and LL/Cr ratios were deemed accurate in finding tumor grade, with LL/Cr being particularly associated with high-grade tumors. In conclusion, MRS can be a valuable tool in grading brain tumors, with an accuracy of up to 88%. Using both short and intermediate TEs together achieves greater accuracy than using each TE separately. The LL/Cr, Cho/Cr, Cho+Cr/NAA and Cho/NAA ratios can be employed to differentiate between low and high-grade tumors.

Brain tumors are challenging to diagnose because patients frequently display vague symptoms that are indicative of less serious illnesses. Brennan et al. conducted a clinical feasibility study to evaluate the efficacy of a spectroscopic liquid biopsy tests for the triage of patients with vague symptoms that might be suggestive of a brain tumor, as well as for brain imaging [20]. Blood samples from 385 individuals were used in the test, which had a 91% sensitivity and 80% specificity for predicting the existence of glioblastoma, the most prevalent and severe brain tumor. The present symptom-based referral criteria could be enhanced by these levels of accuracy, and the evaluation and diagnosis of symptomatic individuals with suspected brain tumors could be sped up. As well as Deep Learning used in Lung Alignment recognition creates good results in that recognition and classification problems [21]. The brain tumor patients are increasing day by day for that problem the forecasting model can be used for predicting cases like BIFM (Big-Data Driven Intelligent Forecasting model for covid-19) by Sujata et al [22].

Omuro et al. discuss the challenges of accurately diagnosing brain tumors due to the similarity of their symptoms with those of other neurological diseases [23]. They highlight the potential of new diagnostic techniques like MRI, SPECT, and PET scans, as well as histological tools like immunohistochemistry and molecular genetics analysis. However, they emphasize that no technique can achieve 100% accuracy and clinical judgment is still required. The authors suggest that communication between different specialists is critical to ensure a successful outcome.

## B. BRAIN TUMOR SEGMENTATION

A convolution neural network (CNN) for segmentation of brain neoplasm on BRATS 2015 dataset, which consists of multiple Convolutional operations, pooling operations, and normalization operations for finding efficient features, is proposed in [24]. Using this we find a mapping between the input and output by adding some non-linearity. The features are collected from each Convolutional network, and these combine features are given to random forest model to train the classifier. By using the random forest classifier, they obtained 67% accuracy and 2.9% loss on the training data.

The dense neural network is used for pixel-wise prediction in images. A lightweight dense neural network was used by Amin et al. in 2018, on ISLES and BRATS dataset for brain neoplasm segmentation [25]. On Flair data, 99.8% dice index is achieved for segmentation. Whereas 98% dice index on T2 weighted data and 97.4% on T1 data in 5.502 s and 98.65% accuracy is achieved. 95.4% dice is attained on T1-weighted contrast-enhanced data.

Numerous computer-aided diagnosis systems are utilized for detection, classification and segmentation. Similarly, a Computerized Technique (CAT) is used by [26], to localize the neoplasm in brain MRI data using different machine learning and image processing techniques, irrespective of its modalities. The technique consists of 3 phases discrete

wavelet transform with PCA, Tri-level thresholding based on Social Group Optimization and the watershed segmentation algorithm. On BRATS 2013 data, the accuracy of 95.74%, sensitivity of 99.93% and specificity of 90.67% was accomplished.

An architecture consisting of Convolutional neural network for classification and region based CNN, called R-CNN, is presented by [27]. The boundary of the neoplasm is contoured for segmentation by Chan-Vese segmentation algorithm. The segmentation technique achieves the accuracy of 0.94%.

A Convolutional neural network is proposed for automation, classification and segmentation of brain neoplasm [8]. The proposed technique works similarly to capsule neural networks (Caps Nets), and there is no need of pre-processing of the dataset. The results show that the segmentation dice index score on Figshare dataset is 82%.

A two-level approach is presented for-brain tumor classification and segmentation [28]. Here, neoplasm is classified with machine learning algorithm and then image processing technique is used for neoplasm region extraction. For this purpose, 7 different methods for texture feature extraction are used [24]. These seven algorithms are K-nearest neighbors (KNNs), random forest (RF), support vector machines (SVMs), binary decision trees (BDTs) and many other ensemble learning techniques. The hybrid technique obtains a dice index of 90.16%.

The various approaches discussed above are used for brain tumor classification and detection. But all the approaches are applicable to the one problem classification or segmentation. This paper proposed a methodology for classification and segmentation. The proposed novel VS-BEAM (Voting Based Semi-Bayesian Ensemble Voting Mechanism) is highly efficient regarding accuracy, recall, F1 score and the latest framework. As well as for segmentation purposes, the Convolutional neural network-based Autoencoder is used to detect the segment and tested on the BraTS2015 dataset.

## III. PROPOSED METHODS

### A. DATASET

The T1-weighted, contrast-enhanced brain neoplasm MRI dataset is acquired from the Figshare platform. The experts provide image labels and tumor masks in the proposed research. The MATLAB file contains three things in one file. Firstly, the image is present in the file. Secondly, the border of the tumor (boundary), and thirdly, the binary mask of the corresponding MRI image to date, the TIW-CE brain MRI images are almost 3064 in number.

Three types of brain tumors exist in this dataset, whose names are meningioma, pituitary and glioma. A contrast agent is used in the T1W-CE modality to visualize brain vessels and provides these benefits: 1) necrotic and active neoplasm areas are properly visible; and (2) the appearance of tumor borders is brighter [29]. The input MRI sequences contain images of size  $512 \times 512$  pixels and their corresponding masks in the form of a binary image.

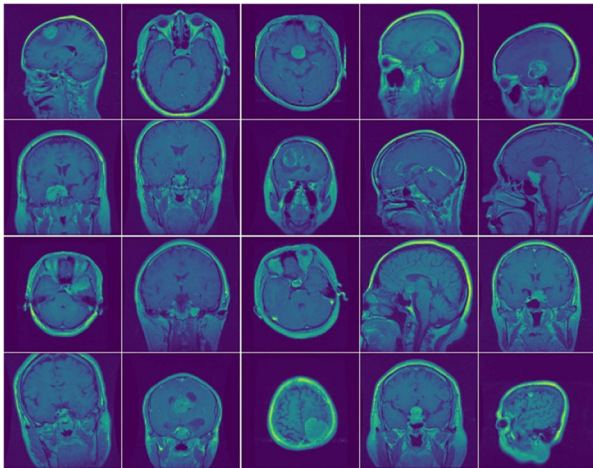


FIGURE 1. Brain MRI dataset.

TABLE 1. Training and testing samples.

Types of Tumors	Meningioma	Glioma	Pituitary
Total data	708	1426	930
Training Data	643	1313	844
Testing Data	65	113	86

In mask, the region containing the tumor is denoted by 1's or 0's. The dataset contains coordinates of the neoplasm border at  $x_1$ ,  $x_2$ ,  $x_3$ , and  $x_4$ . These points are used to detect the tumor in the MRI images as a whole. Fig. 1 shows a sample of the dataset.

The Table 1 shows the Total data samples as well as Training data and testing data of all three types of tumors.

The deep learning approach is the most precise method for classifying and segmenting brain tumors using MRI. The proposed architecture consists of multiple learning techniques for classification, and the methodology includes two phases: classification and segmentation. The proposed method's overview is depicted in Fig 2.

The main purpose of pre-processing is to improve the images to make it applicable for the VS-BEAM model. This enhances the performance of the model. Dataset images and their corresponding masks were extracted from MATLAB files and then converted into JPEG and PNG in array format. The images were resized to  $128 \times 128$ . Brain MRI images are resized, and then normalized using Eq. (1). Range of the pixel is between 0 and 1.

Let 'I' represent the input image having a size ( $m \times n$ ) and  $I_{norm}$  represent the normalized MRI. Then we have Eq. (1) as:

$$I_{norm} = \frac{(I - \min(I))}{(\max(I) - \min(I))} \quad (1)$$

where  $I_{norm}$  in Eq.(1) is the normalized images,  $\min(I)$  &  $\max(I)$  mean minimum and maximum pixel value of in image.

## B. PHASE 1 TUMOR CLASSIFICATION

A total of 3064 T1 weighted contrast-enhanced MR images were used [29]. The dataset contains three types of cancerous and noncancerous tumors such as 1) Meningioma, 2) Glioma and 3) Pituitary tumor. The MRI images' sizes differ; therefore, the images were resized into  $(128 \times 128)$  and then rescaled by 255 to get all the values between 0 and 1. After pre-processing, the training and testing samples are separated. The dataset was split into 90:10 i.e., 90% for training and 10% for testing. The classification process comprises four sequential stages: Squeeze and Excitation Attention, Bayesian Learning, Ensemble learning and voting mechanism.

## C. VSBEAM (VOTING BASED SEMI-BAYESIAN ENSEMBLE ATTENTION MECHANISM) ARCHITECTURE

A Deep Convolutional Directed Acyclic Graph Neural Network is proposed in this research work. It is a custom build model which consists of multiple learning strategies.

The architecture consists of 3 stages.

### 1) SQUEEZE AND EXCITATION SPATIAL ATTENTION

The squeeze and excitation network was published in 2018 by Hu et al. [30]. The task is to scale each feature map by adding weight parameters, and this process is also known as the dynamic feature-wise recalibration mechanism.

The squeeze and excitation mechanism consists of two parts; squeeze and excitation. The data is initially squeezed to a single value using a pooling layer. Afterwards, fully connected layers are used. The first dense layer consists of  $n$  ratio neurons where ratio is a hyper parameter. Second layers consist of  $m$  number neurons where  $n$  is the number of feature maps. Sigmoid function is applied to the last dense layer as it is scaling factor for each feature map. Then the weight is multiplied by the corresponding feature maps to get scaled features. Lastly, the rescaled channels move to next part of the network.

### 2) ENSEMBLE LEARNING & VOTING MECHANISM

Ensemble learning is a generic meta-approach to machine learning that aims to improve predictive performance by combining the predictions of multiple models. Any machine learning challenge aims to identify a single model that can predict the best result. Ensemble approaches consider a wide range of models and average those models to get one final model instead of creating one model and hoping that this model is the best/most accurate predictor. Ensemble model classification proposes a base machine learning model combination, combining the ensemble model with the majority voting technique. The voting mechanism is used to find the majority vote, and the classification is carried out on the basis of the majority class. For instance, if we have  $m$  models then  $p_1, p_2, p_3, \dots, p_m$  predictions for  $m$  models are obtained.

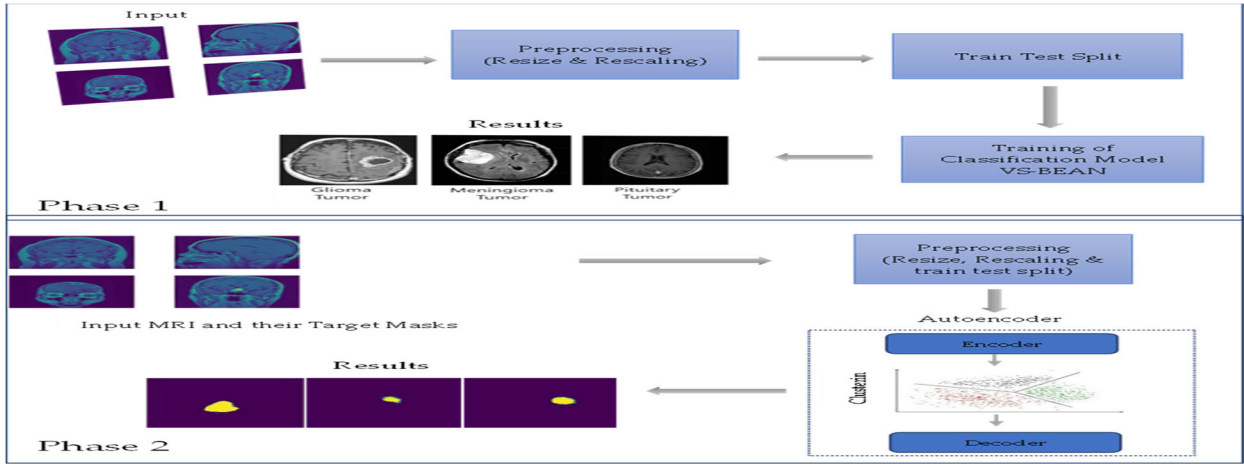


FIGURE 2. Overview of proposed VS-BEAM model.

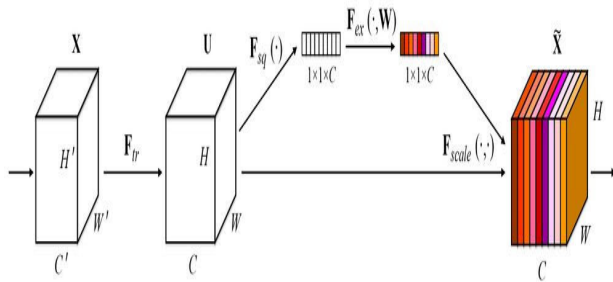


FIGURE 3. Squeeze and Excitation Spatial Attention Diagram source ([30]).

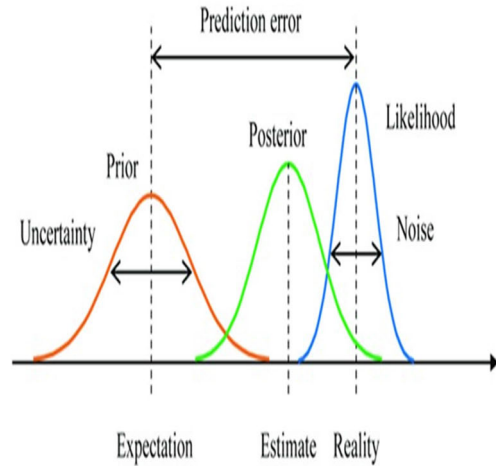


FIGURE 4. Bayesian Learning source ([31]).

### 3) BAYESIAN LEARNING

Bayesian learning is based on Bayes theorem. In the case of data, the probabilities of different events are calculated by prior knowledge. As it is desired to maximize the posterior distribution, thus, if D is data, a question arises: What value of  $\theta$  will maximize the probability of  $\theta$  given D? Formally, we get

$$\hat{\theta}_{MAP} = \underset{\theta}{\operatorname{argmax}} \frac{P(D|\theta) P(\theta)}{P(D)} \quad (2)$$

$P(D|\theta)$  is the Likelihood of the data,  $P(\theta)$  is the prior distribution and  $P(D)$  is the evidence.  $\hat{\theta}_{MAP}$  is the posterior distribution that only depends on  $P(D|\theta)$  and  $P(\theta)$ . When it comes to dealing with uncertainty in predictions, Bayesian statistics provide a solid framework that other methods often lack. Uncertainty of this sort results from a lack of training data or outliers in the test data. Fig. 4 depicts Bayesian learning.

Initially, we combine Stacked Convolutional Layers with Squeeze and Excitation Attention. We use a convolutional layer with 64 filters of size  $3 \times 3$ , the padding is same and relu activation functions. Next, MaxPooling2D layer for feature reduction is used and some invariance in architecture is included with  $2 \times 2$  strides. After the two simple layers, we use

Squeeze and Excitation Spatial Attention to give each channel the right amount of importance. After applying channel-wise attention, we add two more combinations of convolutional layers with 32 filters of size  $3 \times 3$  and activation relu and MaxPooling2D with stride of  $2 \times 2$ . Afterwards, we add latten layer to make a single dimensional Vector. This is portrayed in Fig. 5.

### 4) ENSEMBLE MODEL 1

In the second stage, we solve the problem using three different ways: three-headed binary classification, multi-class classification and Probabilistic Bayesian Learning. In the first step in second stage, we solve the problem with binary classification using one hot encoding. This helps to reduce the biasness, as we have 3 binary classification problems. We build a simple 2-layer Neural Network which comprises

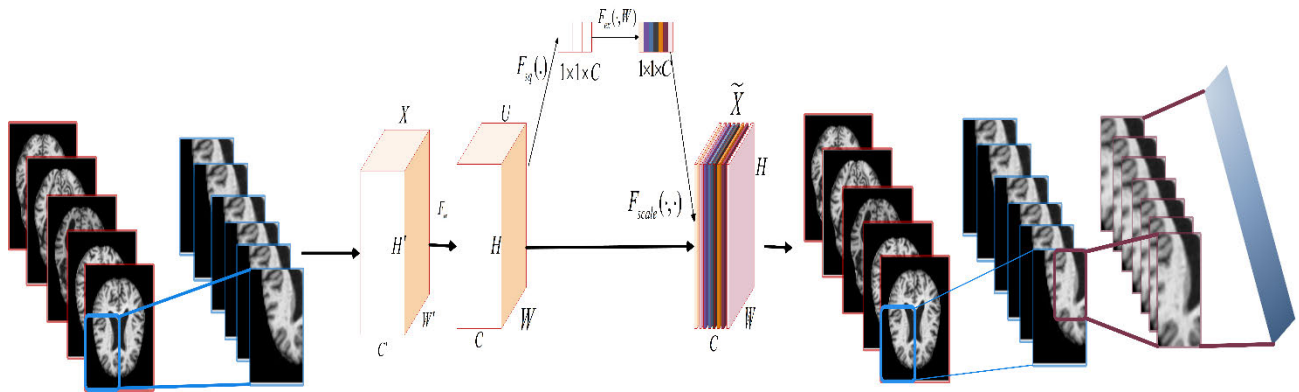


FIGURE 5. Proposed Attention inspired feature extractor.

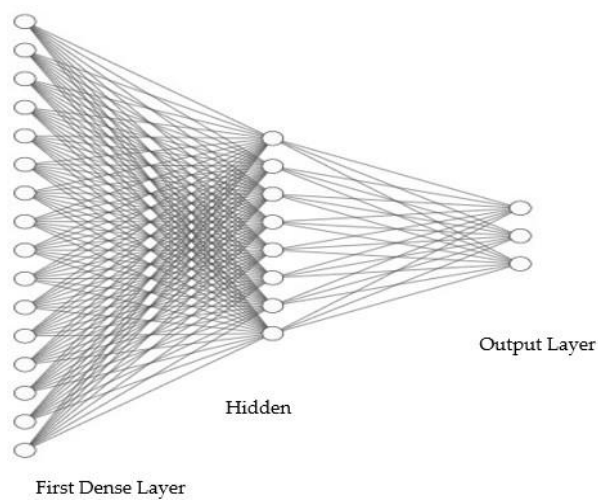


FIGURE 6. Ensemble model 1.

of three layers for output. The output of the previous stage is input for the next stages.

5) ENSEMBLE MODEL 2

Fig. 7 depicts the second step in the second stage, multi-class classification using the features extracted from the first stage. Here, 2 layers simple Neural Network is used with 256, 64 neurons in each layer.

6) ENSEMBLE MODEL 3

The second stage’s third and last step is addressing the multi-class categorization issue with Bayesian Learning. The importance of this approach is to model uncertainty. In this step, we use Bayesian Dense layers for minimizing loss using log-likelihood and Kullback-Leibler Divergence. Finally, we have one hot layer which learns the data’s probability distribution. Fig. 8 illustrates Ensemble model 3.

In the third and final stage, we take feedback from all the three models and find the majority-voted class. The voting mechanism is shown in Fig. 9. We convert the one hot

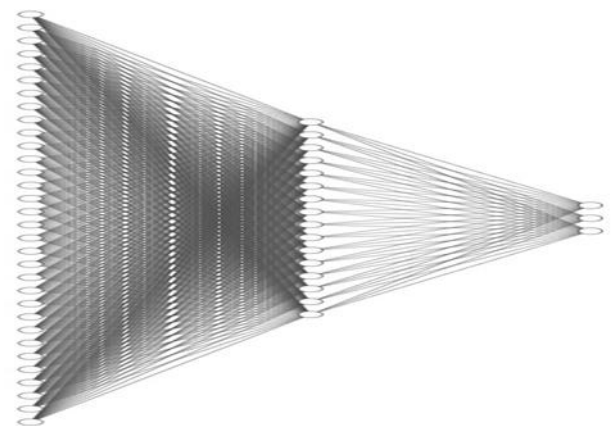


FIGURE 7. Ensemble model 2.

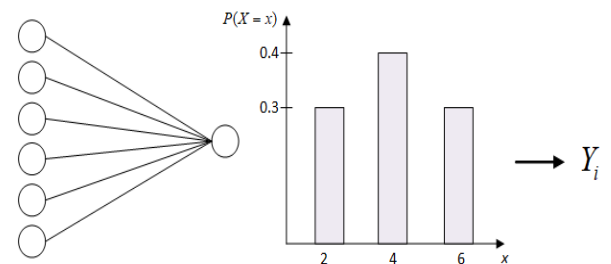


FIGURE 8. Ensemble model 3.

encoded output to a multi-class array and then take the mode of three different predictions for each instance.

Finally, all the stages and ensemble models in a single architecture are combined, which is termed “VS-BEAM,” illustrated in Fig. 10. Initially, the convolutional operations are applied to the input to extract features. Next, a Squeeze and Excitation Attention block is embedded to scale the feature so that the contribution of each feature is according to its importance. The data is then passed through two convolutional layers and a pooling layer block to extract features efficiently. After the optimal features are extracted, the features are sent to three different ensemble learners for



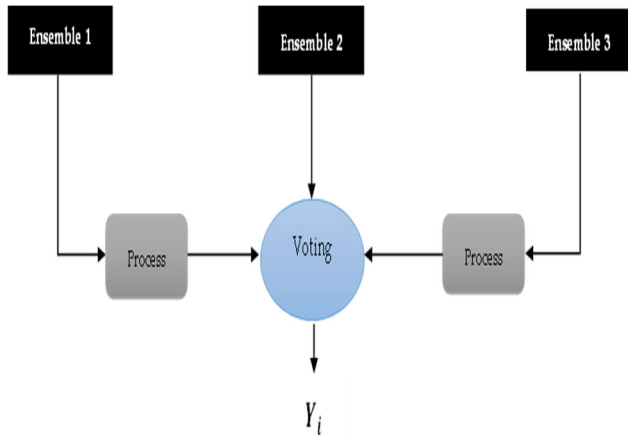


FIGURE 9. Global voting mechanism.

training. First, the ensemble model solves the multi-class problem as a binary problem by one hot encoding the target. As a result, data bias is reduced. The second ensemble model simply solves the problem as a multi-class classification task. The third ensemble model uses Bayesian learning to model uncertainty and learn the probability distribution of data. A 3D random variable is used for modeling distribution. Lastly, a voting mechanism to predict the actual output is used.

The above architecture shows that the squeeze & excitation attention combined with CNN enhanced the performance by extracting efficient features via scaling each feature map with some weight  $w$ . Equation A shows the process mechanism.

$$\begin{aligned}
 X(w, h, c) &\rightarrow F_{\text{squeeze}}(X) \rightarrow F_{\text{excite}}(X) \rightarrow W(1, 1, c) \\
 * X(w, h, c) &\rightarrow (w, h, c') \tag{A}
 \end{aligned}$$

where  $X$  is input and  $(w, h, c)$  shows the shape of data,  $F$  of squeeze is the squeeze operation, and after squeezing, we perform the excitation operation (representing  $F$  of excitation) and multiply weights with each feature map (channel). The whole process is for feature extraction. After this part, classifiers are used to predict the brain tumor in MRI. We use mode as the aggregation function written as in equation B

$$\text{Label} = \text{MODE}(C_1(\text{Features}), C_2(\text{Features}), C_3(\text{Features})) \tag{B}$$

This is our main working scenario where the  $C_1, C_2$  and  $C_3$  are classifiers, Features are the extracted features and MODE is the aggregation function.

**D. PHASE 2: SEGMENTATION OF TUMOR**

Segmentation is localizing the brain neoplasm in the given contrast-enhanced magnetic resonance images. We use a convolutional autoencoder to localize the abnormalities in brain MRI to create the mapping between images and masks.

*The Encoder:* The encoder consists of stacked convolution layers (in the case of images) for efficient feature extraction. Then the features are compressed in low dimensional

using nonlinear transformations. In this manner, the actual high-dimensional input data is encoded into low-dimensional data.

$$\Phi : \chi \rightarrow Z \tag{3}$$

$\Phi$  represents the encoder architecture, where the arrow between  $\chi$  to  $Z$  describes the encoding of images from spatial space to latent space. Where  $\chi$  are images in spatial space and  $Z$  is the encoded embedding in latent space.

*The Decoder:* The decoder consists of convolution and dense layers which take the output of encoder as an input and reconstruct the actual target (input). The task of the decoder is to recreate the high-dimensional actual input from the transformed (or compressed) low-dimensional representation.

$$\psi : Z \rightarrow \chi \tag{4}$$

The  $\psi$  represents the decoder in autoencoder. In this phase the embedding in latent space ( $Z$ ) map to actual images in spatial space ( $\chi$ ). The Decoder part reproduce the images from compressed embedding.

*Autoencoder:* Autoencoder is a combination of two neural networks, encoder and a decoder [32]. The task of the encoder is to represent the information in merely a few parameters in low dimensions (compressed version of actual data). Then the decoder used the encoded information to decode the actual target (input). Convolutional neural networks are used for better feature extraction using spatial information. As we discussed earlier, CAE is a combination of encoder and decoder; first, data is encoded and then decoded by minimizing the loss function. A CAE will be implemented, including convolutions and pooling in the encoder and deconvolution in the decoder. Compared to the autoencoder with fully connected layers, the convolutional autoencoder does better encapsulates the underlying patterns in the pixel data.

$$\psi, \Phi = \text{arg}_{\psi, \Phi} \min ||X - (\Psi \circ \Phi) X||^2 \tag{5}$$

$(\Psi \circ \Phi) X$  describe the encoding and then decoding of data from spatial to latent space and then latent to spatial space. Its mean that  $(\Psi \circ \Phi) X$  is equal to  $X$ . Our loss function is written as  $||X - (\Psi \circ \Phi) X||^2$ . We want to minimize the difference between  $X$  and the predicted output  $(\Psi \circ \Phi) X$  by optimizing the parameters of both encoder  $\Phi$  and decoder  $\Psi$ .

**1) SEGMENTATION USING CONVOLUTIONAL AUTOENCODER (AE)**

Firstly, we take an input image of size  $128 \times 128 \times 1$  and then apply a convolutional operation with  $3 \times 3$  sizes of 16 filters and RELU activation. Next, a max pooling layer with stride  $2 \times 2$  is applied to reduce the parameters. Then we apply one convolutional layer with 8 filters of size  $3 \times 3$  and max pooling with stride  $2 \times 2$  once more.

The output is flattened and given to a dense layer for dimensionality reduction. The main task of an encoder is to compress data and perform clustering to reduce latent space. The latent space data is provided to the decoder to reconstruct

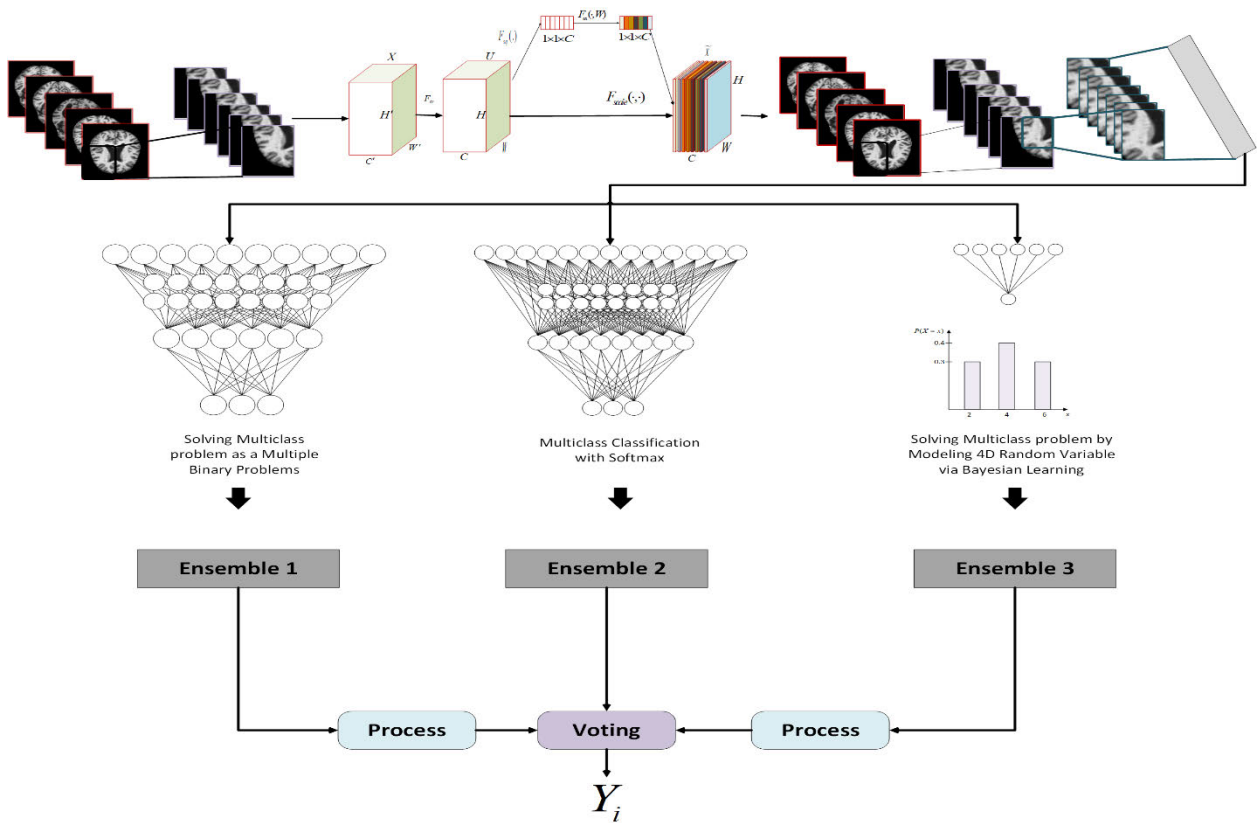


FIGURE 10. Proposed VS-BEAM model.

the input again. Brain MR Images are given as input, and the output is compared with the corresponding masks. So, it creates a mapping between the actual input image and the mask. As a result, if we give the image, we get the mask built with images.

The task of the autoencoder is to learn/generalize the distribution of input and target data and minimize the difference between them. The autoencoder in this work is made up of 11 layers: 4 deconvolution layers, 2 dense layers, and up-sampling and reshape layers. First, we take input from a decoder of size 2, which is the size of latent space. We use a dense layer with 128 neurons, and then we have a reshaping layer whose task is to reshape the size of 128 into  $4 \times 4 \times 8$ . Fig. 11 depicts the convolutional autoencoder.

Next, two deconvolutional layers are applied with 32 and 16 filters of size  $3 \times 3$ . An up-sampling layer is used to increase the parameters. Again, we have two deconvolutional layers applied with 16, 8 filters of size  $3 \times 3$  and a sampling layer. After these blocks, we use a flat and dense layer with  $128 \times 128$  neurons. Next, we reshape the size to  $128 \times 128$ . Segment is learned by comparing the input image with the actual mask. Now, a dense layer at the end of the decoder is not a better idea, but nevertheless, it outperforms the existing segmentation models with a dice index of 96.28.

For calculating loss, binary cross entropy is used and for performance measurement we use both the dice index metrics and accuracy.

The task of encoder is to encode high-dimensional data to lower-dimensional representation. In mathematical notation, the transformation is written as:

$$z = \sigma(Wx + b) \tag{6}$$

$\sigma$  represents any transformation to convert image from one space to other space called latent space. On the other hand, the decoder network is also a neural network whose task is to take the output of the encoder as input and recreate the actual input from the compressed form. The encoder and decoder are two different networks. Encoding and decoding processes are also termed “nonlinear transformations” applied to data. The equation is written as

$$x' = \sigma'(W'z + b') \tag{7}$$

where the  $z$  is output of encoder (encoded data or bottleneck),  $\sigma'$  is the transformation function and  $W'/b'$  are the weights & biases of decoder.  $z$  is input to decoder for the reconstruction of actual input or target.

Now, optimal parameters for both encoder and decoder are found by minimizing the loss function. Loss of function is very vital for training the neural network, and gradients of loss functions are used in network training for back propagation procedures. The autoencoder loss function is

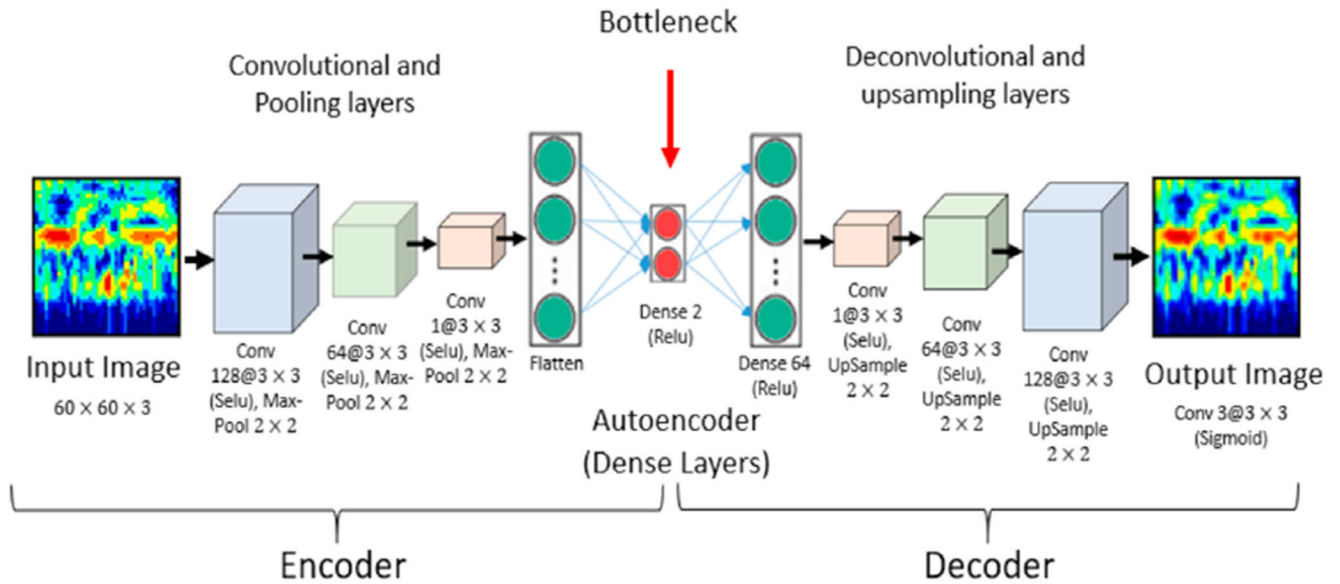


FIGURE 11. Convolutional Autoencoder source ([33]).

defined as:

$$L(x, x') = ||x - x'||^2 = ||x - \sigma'(W'(\sigma(Wx + b)) + b')||^2 \tag{8}$$

Eq. (8) is nothing but explanation of Eq. (5) where x represents actual data (images),  $\sigma$  represents the encoding transformations and  $\sigma'$  represents decoder transformations. So, we can rewrite the equations as  $(\Psi\circ\Phi) X = \sigma'(W'(\sigma(Wx + b)) + b')$ .

#### IV. RESULTS AND DISCUSSION

This section presents a detailed comparison of our work with existing state-of-the-art approaches in brain tumor classification and segmentation. The hyper-parameters of our models are also explained, followed by an evaluation of their performance using various metrics. The section is divided into two parts, where the performance of our algorithm in classification and segmentation tasks are presented separately.

The VS-BEAM algorithm aims to divide brain tumors into three categories using a deep learning model namely meningioma, glioma, and pituitary neoplasms. It was trained on a dataset of T1-weighted contrast-enhanced (T1-W CE) brain MRI images, which are commonly used in medical imaging for diagnosing brain tumors. Each tumor class requires the model to learn unique features for accurate classification. The model has been trained for 300 epochs with 12109330 trainable parameters.

Table 2 provides details of the hyper-parameters used in the VS-BEAM algorithm. Hyper-parameters are not learned during training, but must be set prior to training and include parameters such as the learning rate, batch size, and number of layers in the model. Proper selection of these hyper-parameters is essential for achieving good performance

TABLE 2. Hyper parameter setting for proposed VS-BEAM model.

S/N	Detail	Quantitative values
<b>Voting based Semi Bayesian Ensemble Attention Mechanism (VS-BEAM) model</b>		
1	Layers	20 layers
2	Size of input images	128x128x1
<b>Optimization Parameters</b>		
3	Epoch	300
4	No of classes	3
5	Batch size	88
6	Learning rate	0.001
7	Optimizer	Adam
8	Verbose	False

in the model, as they significantly impact its ability to learn and generalize to new data.

Providing details of the hyper-parameters used in the VS-BEAM algorithm is crucial for transparency and reproducibility of the model’s performance. This allows other researchers to replicate and build upon the work, which can lead to further advancements in the field of brain tumor classification and segmentation using deep learning.

The VS-BEAM model is evaluated and analyzed by the following metric: The F1 score, accuracy, recall, and precision are the key measures for the efficiency and effectiveness of the proposed model.

$$Accuracy = \frac{(TP + TN)}{(TP + FP + TN + FN)} \tag{9}$$

$$F1 - score = \frac{2 * TP}{(2 * TP + FP + FN)} \tag{10}$$

$$Recall = \frac{TP}{(TP + FN)} \tag{11}$$

**TABLE 3.** Comparison of performance.

Author's	Year	Model	Accuracy	Precision	Sensitivity	Specificity
Sri Ramakrishnan [4]	2019	SVM	97.49	-	96.43	98.40
Tanvi Gupta [7]	2017	SVM without PCA	88	-	84	92
Zar Nawab [34]	2019	VGG19	94.82	89.52	94.25	94.69
Lokesh Kumar[9]	2021	ResNet50+ global average pooling	97.48	97.40	97.20	-
Deepak[35]	2019	GoogleNet	97.10	-	97.60	98.96
Cheng[36]	2015	GLCM and BoW model	91.28	-	89.90	95.70
Shaik[37]	2021	MaNet	96.51	96.14	95.99	94.52
Dillip[10]	2022	Dense EfficientNet	98.78	98.75	98.75	-
Soheils[13]	2023	2D CNN	96.47	94.75	-	-
El Wahab[15]	2023	BTC-fCNN	98.63	97.44	97.57	98.82
Rasool[16]	2023	SN-FT	96.5	97	96.8	-
Zhang[17]	2023	ELM	93	-	-	-
<b>Proposed</b>	<b>2023</b>	<b>VS-BEAM</b>	<b>98.86</b>	<b>98.44</b>	<b>97.00</b>	<b>99.45</b>

**TABLE 4.** Comparison with non-ML approaches.

Author's	Year	Model	Accuracy
Naser[19]	2016	TEs	88
Brennan[20]	2021	spectroscopic liquid biopsy	80
<b>Proposed</b>	<b>2023</b>	<b>VS-BEAM</b>	<b>98.86</b>

$$Precision = \frac{TP}{(TP + FP)} \quad (12)$$

where the terms in above equations are defined as:

TP: true positives

TN: true negatives

FP: false positives

FN: false negatives

Table 3 provides a comparison of the performance of the proposed VS-BEAM algorithm with other state-of-the-art models for brain tumor classification. The analysis reveals that the VS-BEAM model has the highest accuracy and specificity score when compared to other models.

The Table 4 provides a comparisons of the proposed VS-BEAM with non-ml approaches for brain tumor classification. From comparison we have identified that proposed scheme perform well as compare to other mode.

For comparison purpose we have used the last eight year data of brain tumor classification. From all the studies we identify that VS-Beam model perform well (Highest True Negative Rate (TNR)) among all other considered in comparison. The TNR represent that how the model accurately identify the negative cases refers to non-tumor in our case. The maximum TNR score represent that VS-BEAM model correctly identify negative cases less as compare to positive cases.

Table 5 presented the proposed VS-BEAM model results of class-specific evaluation. Furthermore, these results are in the form of precisions and F1-scores against three classes of tumors such as glioma, meningioma and pituitary. From

**TABLE 5.** Class-specific evolution of VS-BEAM model on 3 types of cancerous type.

Class	Precision	Sensitivity	F1-score
Glioma	98.00	100	99.00
Meningioma	98.0	97.00	98.00
Pituitary	100	99.00	100
Weighted Avg	100	99.00	99.00

the results we have identified that the proposed model performed extraordinary against all of tumor classes. In three classes the pituitary class f1 score is highest one. Furthermore, the proposed model used semi-Bayesian framework, which product the slight variation in final results. There are continues changes in weights during prediction task which create impact on final prediction task.

Nevertheless, due to the ensemble approach employed by the model, it consistently delivers promising overall results.

The evaluation specific to each tumor class offers valuable insights into the performance of the VS-BEAM model for individual classes.

The above results give an opportunity for further improvements and to can also use this result for comparisons purpose to existing techniques. Furthermore, from the results we have also identify that the proposed model used for the treatment of brain tumor.

Figure 12a represent the overall loss which represent the continuous decrease in loss which representing that the proposed model learning behaviors during training. The Figures 12b, the proposed model accuracy is presented.

The accuracy measurements displayed in Figure 12b correspond to the accuracies of Glioma, Pituitary, and Meningioma obtained from ensemble model 1. The accuracy of the remaining two ensemble models (the multi-class and Bayesian ensemble models) is represented by the combined accuracy and Bayesian accuracy, in contrast. It is clear that the model achieves high and consistent accuracy because the loss continually lowers with time. This provides positive indication

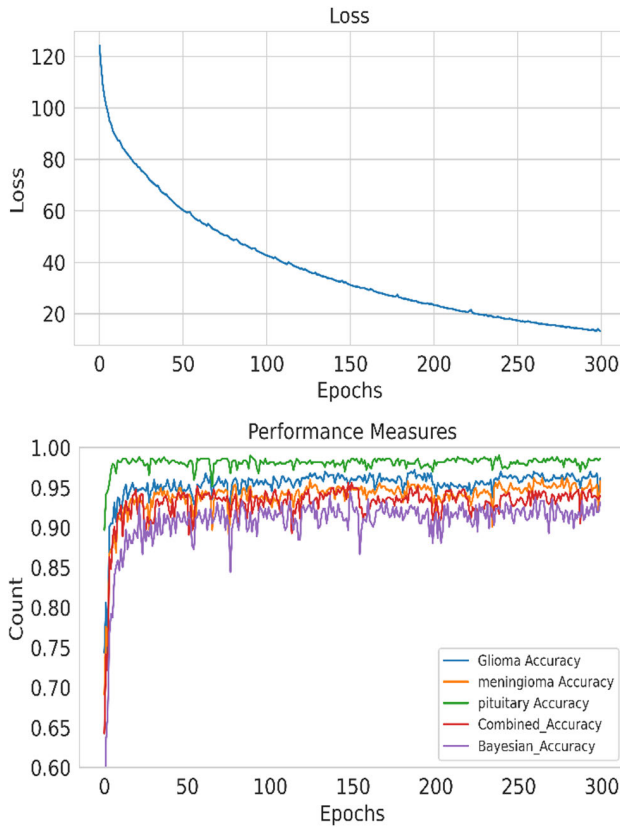


FIGURE 12. a, b: Overall loss and ensemble accuracies & losses.

that the model is correctly classifying brain tumors while effectively learning the relevant features.

Furthermore, the figure 12a illustrates the outcomes of three ensemble architectures, which involve the combination of multiple models to enhance the overall performance. The figure 12b shows that as time passes, the architecture is able to learn optimal parameters, leading to improved performance. This illustrates the VS-BEAM model’s ability for learning from new information and adjusting to it, which is essential for accurate brain tumor classification.

Different characteristics of the model can be taken into account when determining the complexity of a deep learning model. Several popular techniques for evaluating a deep learning model’s complexity are listed below:

1. No of Parameters
2. Depth of Model
3. Computational Complexity

The number of layers, neurons, parameters, and input data size are only a few of the elements that affect how complex a deep learning model is. The model in the current case has 12.10933 million parameters, which is a high number and may add to its complexity. The model also features a deep design with 20 layers, which can add to its complexity. We utilize the Colab T4 GPU for training, with an average duration of 3 seconds per epoch for training and validation on

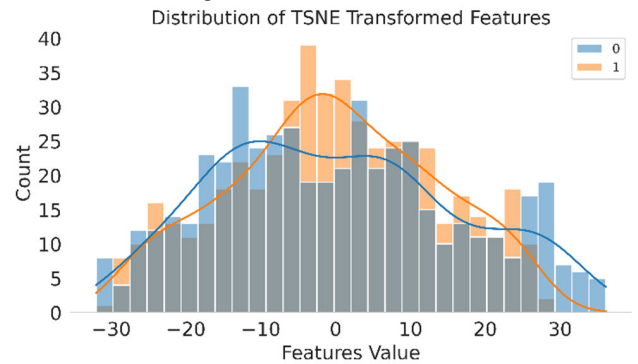


FIGURE 13. Distribution of Features (TSNE).

the testing data. The inference time for the model is estimated to be around 2 seconds.

The size of the input data, in this example  $128 \times 128 \times 3$ , might also have an impact on the model’s complexity. If the input data size is large, it can require more resources and training time, increasing the model’s complexity further. The complexity of a deep learning model can be assessed based on its number of parameters, computational complexity, and memory requirements. This model is quite complex and may require substantial computational resources and memory, especially when working with large datasets.

After training a VS-BEAM model, we need to access the features from the internal layers of the network in order to visualize their distribution. However, these features are often high-dimensional, making it difficult to visualize them effectively. In our case, the dimensionality of the features was approximately 30752, which required the use of feature reduction techniques.

Two common feature reduction techniques are TSNE and PCA [38], [39]. With the help of the TSNE approach, high-dimensional features can be compressed into a two-dimensional space to improve their visual interpretation. On the other hand, PCA splits features into principle components, which are orthogonal components. These elements allow for data visualization in a lower-dimensional space and capture a significant portion of the variation in the original features.

With the use of these feature reduction approaches, we may see the distribution of reduced features and learn more about the structure and arrangement of the features in a lower-dimensional space. These plots are very useful for examining the features behavior and how it relates to the target variable. The transformation of features using both PCA and TSNE techniques produced the visual representations of the feature distribution shown in Figures 14 and 15.

The fact that the feature space in our situation has a lot of dimensions was mentioned in our earlier discussion. We used a feature importance-based strategy in addition to PCA and TSNE to tackle this problem. This strategy involves evaluating each feature’s importance and choosing to plot only those that have the most impact on the analysis.

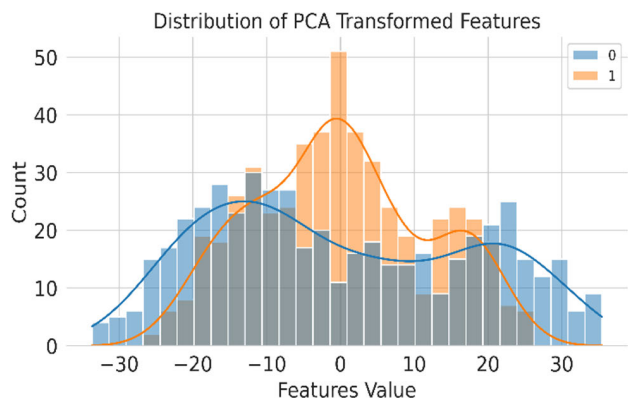


FIGURE 14. Distribution of features (PCA).

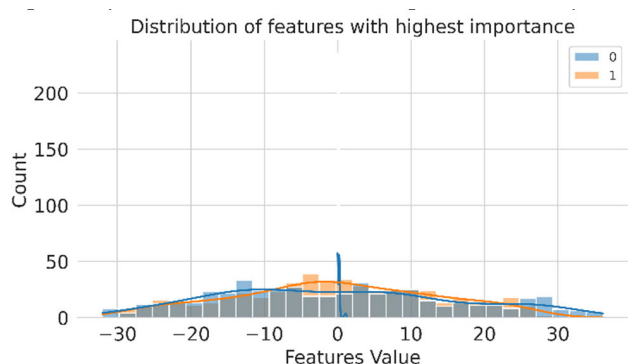


FIGURE 15. Features with importance.

For the features with high importance, we observed that none of them had an importance value exceeding 0.37. Consequently, we chose to visualize the distributions for importance values greater than 0.2, 0.3, and the highest value of 0.37, as demonstrated in Figure 15.

To calculate the importance values for each feature, we used Lasso Regression [40]. Following model training, the resulting coefficients were used to determine the significance values for each feature. As a result, we were able to rank each feature according to their importance and narrow our focus to just visualizing the distribution of the features that are most important.

The distribution of features depending on relevance is shown in Figure 16. We were able to focus on the most important features and understand their distribution better using this approach. The model’s performance can be enhanced by using this information, which can also provide important new insights into how the features behave.

To examine the relationship between the features after dimensionality reduction with TSNE, we also generate scatter plots between the features in a class-wise manner in Figure 17. This scatter plot helps us understand the correlation between the features and their distribution with respect to different classes.

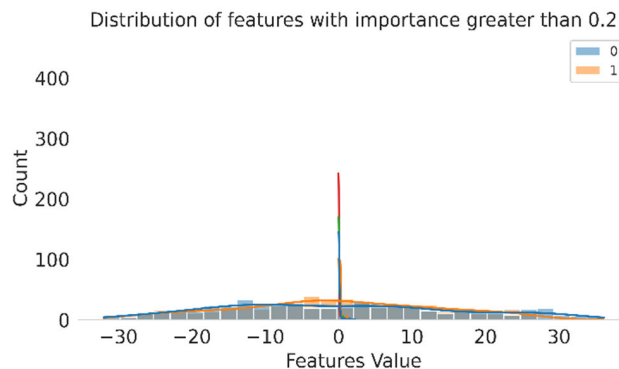


FIGURE 16. Features with high importance.

TABLE 6. Comparison of proposed brain neoplasm segmentation techniques.

Author's	Year	Model	Accuracy
Rao[24]	2015	CNN	67
Rajinikanth[26]	2018	DWT-PCA	95.74
Gunasekara[27]	2019	Chan-Vese	94.57
Kumar[41]	2015	PCA and RBF Kernel	94
Biswajit[28]	2022	Hybrid segmentation	98.40
Proposed	2023	Autoencoder	98.91

*Tumor Segmentation:* For brain tumor segmentation, a convolutional autoencoder is utilized, which is trained on images with dimensions of  $128 \times 128 \times 1$ . This implies that each input image has a single-color channel and a resolution of  $128 \times 128$  pixels. The objective of the autoencoder is to learn a condensed representation of the input image that can be utilized to reconstruct the original image. To accomplish the task of brain tumor segmentation, which entails separating the tumor region from the surrounding healthy brain tissue, the autoencoder is trained. The accuracy metric, which is typically applied to tasks involving image segmentation, is taken into consideration in the process of evaluating the performance of the autoencoder. The high level of precision that the autoencoder possesses is demonstrated by the fact that it can segment brain tumors with an accuracy of 98.91 percent. Table 6 depicts the results of segmentation performed on a variety of different designs, one of which is the recommended Convolutional AutoEncoder (CAE). The examination of the data demonstrates that the proposed mechanism is superior to the previously employed.

In the proposed work, we recommend using a CAE to perform the segmentation of brain tumors. The performance of the proposed work was evaluated by comparing it to other approaches that are already in use. The segmentation results for various architectures, including the proposed Convolutional Autoencoder, are presented in Table 6. According to the findings analysis, the suggested mechanism performs better than the other examined architectures.

Moreover, the proposed Convolutional Autoencoder achieved an accuracy of 98.91% for segmentation, which is the highest among all previously used strategies on the

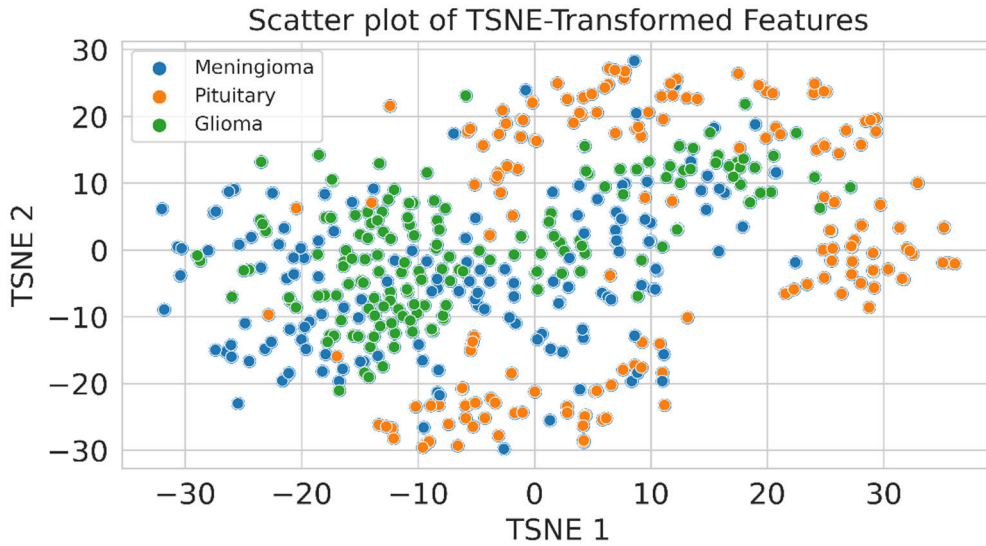


FIGURE 17. Scatter plot of TSET features.

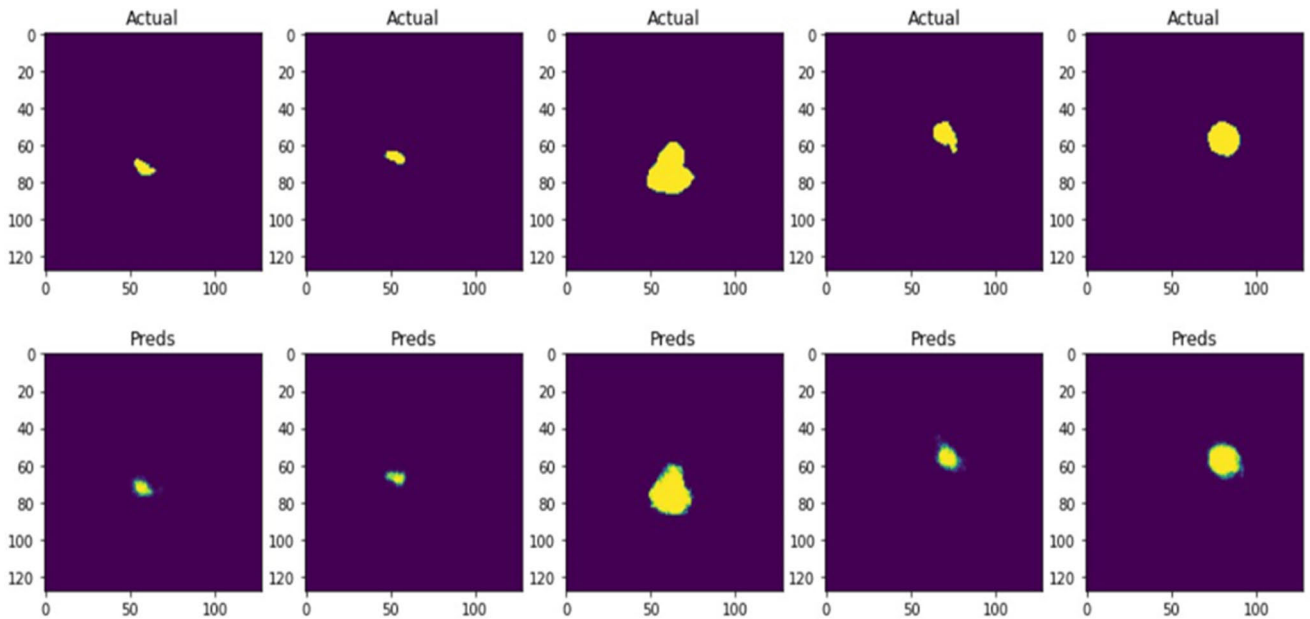


FIGURE 18. Comparison of actual and predictions after segmentation.

brain MRI dataset. This indicates that the proposed model can accurately distinguish the tumor region from healthy brain tissue in the given dataset.

To further illustrate the segmentation results, Figure 18 is presented, which compares the actual and predicted data after segmentation. The figure shows that the proposed Convolutional Autoencoder can segment the tumor region with high precision, as the predicted data closely matches the actual data.

**V. CONCLUSION**

Diagnosing brain tumors is challenging because of their high prevalence, heterogeneity, and non-classical distribution. We proposed a deep learning-based Directed Acyclic Graph

Neural Network algorithm to tackle this problem. This research suggests a novel deep embedding approach for training and predicting classifiers. The anticipated channel attention-based Semi-Bayesian Ensemble Voting Mechanism (VS-BEAM) has very high performance in terms of accuracy and specificity. Based on the proposed idea, the tumors in the brain are detected with high accuracy. The proposed methodology achieves a training accuracy of 100% and a testing accuracy of 98.86%. This research also suggests a Convolutional Autoencoder (AE) for brain neoplasm segmentation purposes with an average accuracy of 98.91%. Brain neoplasm classification and segmentation are performed separately in this research. Reducing the number of parameters, reducing computing time, and enhancing the

overall performance of the architecture are some of the future guidelines.

## ACKNOWLEDGMENT

The researchers would like to acknowledge Deanship of Scientific Research, Taif University for funding this work.

## REFERENCES

- [1] S. A. Nawaz, D. M. Khan, and S. Qadri, "Brain tumor classification based on hybrid optimized multi-features analysis using magnetic resonance imaging dataset," *Appl. Artif. Intell.*, vol. 36, no. 1, pp. 1–10, Dec. 2022, doi: [10.1080/08839514.2022.2031824](https://doi.org/10.1080/08839514.2022.2031824).
- [2] M. Dubol, I. Sundström-Poromaa, and E. Comasco, "P.275 severity of premenstrual dysphoric disorder symptoms correlates with grey matter, volume and brain surface morphology," *Eur. Neuropsychopharmacol.*, vol. 40, pp. 1–10, Jan. 2020, doi: [10.1016/j.euroneuro.2020.09.207](https://doi.org/10.1016/j.euroneuro.2020.09.207).
- [3] M. Nagabushanam, G. S. Nandeesh, and R. Vijayarajeswari, "Detection and localization of brain tumors using fractional Hartley transform and adaptive neuro-fuzzy inference system classification methods," *J. Ambient Intell. Humanized Comput.*, vol. 14, no. 7, pp. 8851–8858, Jul. 2023, doi: [10.1007/s12652-021-03633-8](https://doi.org/10.1007/s12652-021-03633-8).
- [4] P. Sriramkrishnan, T. Kalaiselvi, and R. Rajeswaran, "Modified local ternary patterns technique for brain tumour segmentation and volume estimation from MRI multi-sequence scans with GPU CUDA machine," *Biocybern. Biomed. Eng.*, vol. 39, no. 2, pp. 470–487, Apr. 2019, doi: [10.1016/j.bbe.2019.02.002](https://doi.org/10.1016/j.bbe.2019.02.002).
- [5] M. K. Abd-Ellah, A. I. Awad, A. A. M. Khalaf, and H. F. A. Hamed, "Two-phase multi-model automatic brain tumour diagnosis system from magnetic resonance images using convolutional neural networks," *EURASIP J. Image Video Process.*, vol. 2018, no. 1, pp. 1–16, Dec. 2018, doi: [10.1186/s13640-018-0332-4](https://doi.org/10.1186/s13640-018-0332-4).
- [6] E. I. Zacharakis, S. Wang, S. Chawla, D. S. Yoo, R. Wolf, E. R. Melhem, and C. Davatzikos, "Classification of brain tumor type and grade using MRI texture and shape in a machine learning scheme," *Magn. Reson. Med.*, vol. 62, no. 6, pp. 1609–1618, Dec. 2009, doi: [10.1002/mrm.22147](https://doi.org/10.1002/mrm.22147).
- [7] T. Gupta, T. K. Gandhi, R. K. Gupta, and B. K. Panigrahi, "Classification of patients with tumor using MR FLAIR images," *Pattern Recognit. Lett.*, vol. 139, pp. 112–117, Nov. 2020, doi: [10.1016/j.patrec.2017.10.037](https://doi.org/10.1016/j.patrec.2017.10.037).
- [8] F. J. Díaz-Pernas, M. Martínez-Zarzuola, M. Antón-Rodríguez, and D. González-Ortega, "A deep learning approach for brain tumor classification and segmentation using a multiscale convolutional neural network," *Healthcare*, vol. 9, no. 2, p. 153, Feb. 2021, doi: [10.3390/healthcare9020153](https://doi.org/10.3390/healthcare9020153).
- [9] R. L. Kumar, J. Kakarla, B. V. Isunuri, and M. Singh, "Multi-class brain tumor classification using residual network and global average pooling," *Multimedia Tools Appl.*, vol. 80, no. 9, pp. 13429–13438, Apr. 2021, doi: [10.1007/s11042-020-10335-4](https://doi.org/10.1007/s11042-020-10335-4).
- [10] D. R. Nayak, N. Padhy, P. K. Mallick, M. Zymbler, and S. Kumar, "Brain tumor classification using dense efficient-net," *Axioms*, vol. 11, no. 1, p. 34, Jan. 2022, doi: [10.3390/axioms11010034](https://doi.org/10.3390/axioms11010034).
- [11] S. Ahuja, B. K. Panigrahi, and T. K. Gandhi, "Enhanced performance of dark-nets for brain tumor classification and segmentation using colormap-based superpixel techniques," *Mach. Learn. Appl.*, vol. 7, Mar. 2022, Art. no. 100212, doi: [10.1016/j.mlwa.2021.100212](https://doi.org/10.1016/j.mlwa.2021.100212).
- [12] G. Mustafa, M. Usman, L. Yu, M. T. Afzal, M. Sulaiman, and A. Shahid, "Multi-label classification of research articles using Word2Vec and identification of similarity threshold," *Sci. Rep.*, vol. 11, no. 1, pp. 1–12, Nov. 2021, doi: [10.1038/s41598-021-01460-7](https://doi.org/10.1038/s41598-021-01460-7).
- [13] S. Saeedi, S. Rezayi, H. Keshavarz, and S. R. N. Kalhori, "MRI-based brain tumor detection using convolutional deep learning methods and chosen machine learning techniques," *BMC Med. Informat. Decis. Making*, vol. 23, no. 1, pp. 1–17, Jan. 2023, doi: [10.1186/s12911-023-02114-6](https://doi.org/10.1186/s12911-023-02114-6).
- [14] T. H. Shemanto, L. B. Billah, and M. A. Ibtesham, "A novel method of thresholding for brain tumor segmentation and detection," in *Proc. Int. Conf. Inf. Commun. Technol. Develop.*, 2023, pp. 277–289, doi: [10.1007/978-981-19-7528-8\\_22](https://doi.org/10.1007/978-981-19-7528-8_22).
- [15] B. S. A. El-Wahab, M. E. Nasr, S. Khamis, and A. S. Ashour, "BTC-fCNN: Fast convolution neural network for multi-class brain tumor classification," *Health Inf. Sci. Syst.*, vol. 11, no. 1, pp. 1–16, Jan. 2023, doi: [10.1007/s13755-022-00203-w](https://doi.org/10.1007/s13755-022-00203-w).
- [16] M. Rasool, N. A. Ismail, A. Al-Dhaqm, W. M. S. Yafooz, and A. Alsaedi, "A novel approach for classifying brain tumours combining a SqueezeNet model with SVM and fine-tuning," *Electronics*, vol. 12, no. 1, p. 149, Dec. 2022, doi: [10.3390/electronics12010149](https://doi.org/10.3390/electronics12010149).
- [17] L. Zhang, X. Liu, X. Xu, W. Liu, Y. Jia, W. Chen, X. Fu, Q. Li, X. Sun, Y. Zhang, S. Shu, X. Zhang, R. Xiang, H. Chen, P. Sun, D. Geng, Z. Yu, J. Liu, and J. Wang, "An integrative non-invasive malignant brain tumors classification and Ki-67 labeling index prediction pipeline with radiomics approach," *Eur. J. Radiol.*, vol. 158, Jan. 2023, Art. no. 110639, doi: [10.1016/j.ejrad.2022.110639](https://doi.org/10.1016/j.ejrad.2022.110639).
- [18] R. Hustinx, R. J. Smith, F. Benard, A. Bhatnagar, and A. Alavi, "Can the standardized uptake value characterize primary brain tumors on FDG-PET?" *Eur. J. Nucl. Med. Mol. Imag.*, vol. 26, no. 11, pp. 1501–1509, Oct. 1999, doi: [10.1007/s002590050487](https://doi.org/10.1007/s002590050487).
- [19] R. K. A. Naser, A. A. K. Hassan, A. M. Shabana, and N. N. Omar, "Role of magnetic resonance spectroscopy in grading of primary brain tumors," *Egyptian J. Radiol. Nucl. Med.*, vol. 47, no. 2, pp. 577–584, Jun. 2016, doi: [10.1016/j.ejrm.2016.03.011](https://doi.org/10.1016/j.ejrm.2016.03.011).
- [20] P. M. Brennan, H. J. Butler, L. Christie, M. G. Hegarty, M. D. Jenkinson, C. Keerie, J. Norrie, R. O'Brien, D. S. Palmer, B. R. Smith, and M. J. Baker, "Early diagnosis of brain tumours using a novel spectroscopic liquid biopsy," *Brain Commun.*, vol. 3, no. 2, Apr. 2021, Art. no. fcab056, doi: [10.1093/braincomms/fcab056](https://doi.org/10.1093/braincomms/fcab056).
- [21] A. Kumar, K. Abhishek, C. Chakraborty, and N. Kryvinska, "Deep learning and Internet of Things based lung ailment recognition through coughing spectrograms," *IEEE Access*, vol. 9, pp. 95938–95948, 2021, doi: [10.1109/ACCESS.2021.3094132](https://doi.org/10.1109/ACCESS.2021.3094132).
- [22] S. Dash, C. Chakraborty, S. K. Giri, S. K. Pani, and J. Frnda, "BIFM: Big-data driven intelligent forecasting model for COVID-19," *IEEE Access*, vol. 9, pp. 97505–97517, 2021, doi: [10.1109/ACCESS.2021.3094658](https://doi.org/10.1109/ACCESS.2021.3094658).
- [23] A. M. Omuro, C. C. Leite, K. Mokhtari, and J. Y. Delattre, "Pitfalls in the diagnosis of brain tumours," *Lancet Neurol.*, vol. 5, no. 11, pp. 937–948, 2006, doi: [10.1016/S1474-4422\(06\)70597-X](https://doi.org/10.1016/S1474-4422(06)70597-X).
- [24] V. Rao, M. S. Sarabi, and A. Jaiswal, "Brain tumor segmentation with deep learning," *MICCAI Multimodal Brain Tumor Segmentation Challenge*, vol. 59, pp. 1–4, Oct. 2015.
- [25] J. Amin, M. Sharif, M. Yasmin, and S. L. Fernandes, "Big data analysis for brain tumor detection: Deep convolutional neural networks," *Future Gener. Comput. Syst.*, vol. 87, pp. 290–297, Oct. 2018, doi: [10.1016/j.future.2018.04.065](https://doi.org/10.1016/j.future.2018.04.065).
- [26] V. Rajinikanth, S. C. Satapathy, N. Dey, and R. Vijayarajan, "DWT-PCA image fusion technique to improve segmentation accuracy in brain tumor analysis," in *Microelectronics, Electromagnetics and Telecommunications (Lecture Notes in Electrical Engineering)*, vol. 471. Singapore: Springer, 2018, doi: [10.1007/978-981-10-7329-8\\_46](https://doi.org/10.1007/978-981-10-7329-8_46).
- [27] S. R. Gunasekara, H. N. T. K. Kaldera, and M. B. Dissanayake, "A systematic approach for MRI brain tumor localization and segmentation using deep learning and active contouring," *J. Healthcare Eng.*, vol. 2021, pp. 1–13, Feb. 2021, doi: [10.1155/2021/6695108](https://doi.org/10.1155/2021/6695108).
- [28] B. Jena, G. K. Nayak, and S. Saxena, "An empirical study of different machine learning techniques for brain tumor classification and subsequent segmentation using hybrid texture feature," *Mach. Vis. Appl.*, vol. 33, no. 1, pp. 1–15, Jan. 2022, doi: [10.1007/s00138-021-01262-x](https://doi.org/10.1007/s00138-021-01262-x).
- [29] C. Jun. (2017). *Brain Tumor Dataset*. Figshare. [Online]. Available: [https://figshare.com/articles/brain\\_tumor\\_dataset/1512427](https://figshare.com/articles/brain_tumor_dataset/1512427)
- [30] J. Hu, L. Shen, and G. Sun, "Squeeze-and-excitation networks," in *Proc. IEEE/CVF Conf. Comput. Vis. Pattern Recognit.*, Jun. 2018, pp. 7132–7141, doi: [10.1109/CVPR.2018.00745](https://doi.org/10.1109/CVPR.2018.00745).
- [31] H. Yanagisawa, O. Kawamata, and K. Ueda, "Modeling emotions associated with novelty at variable uncertainty levels: A Bayesian approach," *Frontiers Comput. Neurosci.*, vol. 13, pp. 1–14, Jan. 2019, doi: [10.3389/fncom.2019.00002](https://doi.org/10.3389/fncom.2019.00002).
- [32] W. H. L. Pinaya, S. Vieira, R. Garcia-Dias, and A. Mechelli, "Autoencoders," in *Machine Learning: Methods and Applications to Brain Disorders*. U.K.: Academic, 2019, doi: [10.1016/B978-0-12-815739-8.00011-0](https://doi.org/10.1016/B978-0-12-815739-8.00011-0).
- [33] M. Kaji, J. Parvizian, and H. W. van de Venn, "Constructing a reliable health indicator for bearings using convolutional autoencoder and continuous wavelet transform," *Appl. Sci.*, vol. 10, no. 24, p. 8948, Dec. 2020, doi: [10.3390/app10248948](https://doi.org/10.3390/app10248948).
- [34] Z. N. K. Swati, Q. Zhao, M. Kabir, F. Ali, Z. Ali, S. Ahmed, and J. Lu, "Brain tumor classification for MR images using transfer learning and fine-tuning," *Computerized Med. Imag. Graph.*, vol. 75, pp. 34–46, Jul. 2019, doi: [10.1016/j.compmedimag.2019.05.001](https://doi.org/10.1016/j.compmedimag.2019.05.001).



- [35] S. Deepak and P. M. Ameer, "Brain tumor classification using deep CNN features via transfer learning," *Comput. Biol. Med.*, vol. 111, Aug. 2019, Art. no. 103345, doi: [10.1016/j.combiomed.2019.103345](https://doi.org/10.1016/j.combiomed.2019.103345).
- [36] J. Cheng, W. Huang, S. Cao, R. Yang, W. Yang, Z. Yun, Z. Wang, and Q. Feng, "Enhanced performance of brain tumor classification via tumor region augmentation and partition," *PLoS ONE*, vol. 10, no. 10, Oct. 2015, Art. no. e0140381, doi: [10.1371/journal.pone.0140381](https://doi.org/10.1371/journal.pone.0140381).
- [37] N. S. Shaik and T. K. Cherukuri, "Multi-level attention network: Application to brain tumor classification," *Signal, Image Video Process.*, vol. 16, no. 3, pp. 817–824, Apr. 2022, doi: [10.1007/s11760-021-02022-0](https://doi.org/10.1007/s11760-021-02022-0).
- [38] L. Van Der Maaten and G. Hinton, "Visualizing data using t-SNE," *J. Mach. Learn. Res.*, vol. 9, pp. 1–27, Jan. 2008.
- [39] I. T. Jolliffe and J. Cadima, "Principal component analysis: A review and recent developments," *Phil. Trans. Roy. Soc. A, Math., Phys. Eng. Sci.*, vol. 374, no. 2065, Apr. 2016, Art. no. 20150202, doi: [10.1098/rsta.2015.0202](https://doi.org/10.1098/rsta.2015.0202).
- [40] R. Tibshirani, "Regression shrinkage and selection via the lasso: A retrospective," *J. Roy. Stat. Soc. B, Stat. Methodol.*, vol. 73, no. 3, pp. 273–282, Jun. 2011, doi: [10.1111/j.1467-9868.2011.00771.x](https://doi.org/10.1111/j.1467-9868.2011.00771.x).
- [41] P. Kumar and B. Vijayakumar, "Brain tumour MR image segmentation and classification using by PCA and RBF kernel based support vector machine," *Middle-East J. Sci. Res.*, vol. 23, no. 9, pp. 2106–2116, 2015.



**SYED MUHAMMAD AHMED HASSAN SHAH** was born in Kamra, Attock, Pakistan, in 2001. He received the B.S. degree in computer science from COMSATS University Islamabad, Attock Campus, in 2022. Currently, he is a Research Assistant with the Medical Imaging and Diagnostic Laboratory, National Center of Artificial Intelligence, COMSATS University Islamabad. His research interests include computer vision, medical imaging, natural language processing,

computational quantum field theory, quantum deep learning, graph neural networks, evolutionary optimization techniques, representation theory, and generative adversarial and Bayesian learning.



**ASAD ULLAH** was born in Attock city, Punjab, Pakistan. He received the bachelor's degree in computer science from COMSATS University Islamabad, Attock Campus. His research interests include artificial intelligence, machine learning, computer vision, deep neural networks, recurrent neural networks, and medical imaging analysis.



**JAWAID IQBAL** received the Ph.D. degree from Hazara University, in 2021. He has been teaching at university level for more than nine years. He started his career with the IT Department, Hazara University, Mansehra, in 2013. Meanwhile, he also worked with different universities, such as the Abbottabad University of Science and Technology (AUST), University of Sialkot, and Capital University of Science and Technology (CUST), Islamabad. Currently, he is an Assistant

Professor with the Faculty of Computing, Riphah International University, Islamabad. He has taught various subjects of computer science at bachelor's and M.S. program-levels along with Ph.D. levels programs. He is a member of the Advance Network and Security Research Group, CUST. He has numerous publications in international conferences and journals. His research interests include information security, smart cryptography, cryptanalysis, wireless sensor network security, body sensor network security, smart grid security, VANET security, the IoT security and privacy, and machine learning.



**SAMI BOUROUIS** received the engineering, M.Sc., and Ph.D. degrees in computer science from the University of Tunis, Tunisia, in 2003, 2005, and 2011, respectively. He is currently an Associate Professor with the College of Computers and Information Technology, Taif University, Saudi Arabia. His research interests include data mining, image processing, statistical machine learning, cybersecurity, and pattern recognition applied to several real-life applications.



**SYED SAJID ULLAH** received the master's (M.S.) degree in computer science from Hazara University Mansehra, Pakistan. He is currently pursuing the Ph.D. degree with the Department of Information and Communication Technology, University of Agder, Grimstad, Norway and Villanova University, USA. He is also a Researcher with the National Institute of Standards and Technology (NIST) in the projects (Practical Implementation of Quantum Cryptography and Security Solutions

for Future Internet Architecture Named Data Networking). His research interests include cryptography, network security, information-centric networking (ICN), named data networking (NDN), and the IoT.



**SADDAM HUSSAIN** received the bachelor's degree from the Islamia College, Peshawar, in 2017, and the master's degree from Hazara University Masehra, Pakistan, in 2021. He is currently pursuing the Ph.D. degree with the School of Digital Science, Universiti Brunei Darussalam, Brunei. He has published several papers in well reputed journals, including IEEE, *JISA* (Elsevier), *Cluster Computing*, *Computer Communication*, *IEEE INTERNET OF THINGS JOURNAL*, *CMC*, *Sensors*,

*Mathematics*, *Applied Sciences*, and *Electronics*. His research interests include cryptography, network security, wireless sensor networking (WSN), information-centric networking (ICN), named data networking (NDN), smart grids, the Internet of Things (IoT), the IIoT, quantum computing, cloud computing, and edge computing. He is serving as a Reviewer in reputed journals, including IEEE ACCESS, *International Journal of Wireless Information Networks*, *Scientific Journal of Electrical, Computer, and Informatics Engineering*, and *CMC*.



**MUHAMMAD QASIM KHAN** received the master's degree in computer science from the University of Arid Agriculture, Rawalpindi, Pakistan, in 2011. He is currently pursuing the Ph.D. degree with the Department of Computer Science, University of Engineering and Technology Taxila, Pakistan. He is also working in COMSATS Islamabad, Attock Campus as a Lecture in Computer Science Department. His current research interests include image processing and machine learning.



**YASER ALI SHAH** received the B.S. degree in computer systems engineering and the M.S. degree in computer systems engineering from the University of Engineering & Technology, Peshawar, in 2010 and 2013, respectively, and the Ph.D. degree in computer engineering from the University of Engineering and Technology, Taxila, Pakistan, in 2021. He is currently an Assistant Professor with COMSATS University Islamabad, Attock Campus, Pakistan. He has more than 11 years of experience in teaching and research. His research interests include vehicular ad-hoc networks, machine learning, image and video processing, and bio-inspired algorithms.



**GHULAM MUSTAFA** received the B.S. degree in software engineering from COMSATS University Islamabad, Abbottabad, in 2017, and the M.S. degree (Hons.) in computer science from the Capital University of Science and Technology, Islamabad. He is currently pursuing the Ph.D. degree in computer science with the University of Engineering and Technology, Taxila, Pakistan. He has been associated with academia and industry for the last six years. He is also a Senior Lecturer with the Faculty of Computing, Shifa Tameer-e-Millat University, Islamabad. Previously, he has worked five years with the CS Department, Capital University of Science and Technology, Islamabad, as an Associate Lecturer and a Junior Lecturer. Furthermore, he was with A&F Solution Software House as a Web Frontend Designer and a Backend Developer. Moreover, with academia, he is also an active freelancer from the last four years, doing projects in different languages such as, Python, Java, and C++. In his academic career, he has taught different computer science laboratories, such as the Introduction to Programming Laboratory (C++), Object Oriented Programming Laboratory (C++), Advanced Computer Programming Laboratory (JAVA), Database System Laboratory, Data Structure Laboratory (C++), Computer Communication and Network Laboratory (CNN), and Web Development Laboratory, while as a Junior Lecturer. Moreover, he has also taught different computer science courses such as, introduction to programming, object oriented programming, discrete structure, theory of automata, and software engineering, while as a Senior Lecturer and an Associate Lecturer. He received two gold medals on his first position in Abbottabad Campus and got first position in all seven campuses of CUI for the B.S. degree. He also received the gold medal due to his excellent academic performance in his entire degree duration for the M.S. degree.

• • •